

SPAK-Knockout Mice Manifest Gitelman Syndrome and Impaired Vasoconstriction

Sung-Sen Yang,^{*†‡} Yi-Fen Lo,[‡] Chin-Chen Wu,[§] Shu-Wha Lin,^{||} Chien-Ju Yeh,^{*} Pauling Chu,^{*‡} Huey-Kang Sytwu,[‡] Shinichi Uchida,^{||} Sei Sasaki,^{||} and Shih-Hua Lin^{*‡}

^{*}Division of Nephrology, Department of Medicine, Tri-Service General Hospital, and [†]Graduate Institute of Physiology, [‡]Graduate Institute of Life Science, and [§]Department of Pharmacology, National Defense Medical Center, Taipei, Taiwan; ^{||}Graduate Institute of Medical Technology, National Taiwan University, Taipei, Taiwan; and ^{||}Department of Nephrology, Graduate School of Medicine, Tokyo Medical and Dental University, Tokyo, Japan

ABSTRACT

Polymorphisms in the gene encoding sterile 20/SPS1-related proline/alanine-rich kinase (SPAK) associate with hypertension susceptibility in humans. SPAK interacts with WNK kinases to regulate the Na⁺-K⁺-2Cl⁻ and Na⁺-Cl⁻ co-transporters [collectively, N(K)CC]. Mutations in WNK1/4 and N(K)CC can cause changes in BP and dyskalemia in humans, but the physiologic role of SPAK *in vivo* is unknown. We generated and analyzed SPAK-null mice by targeting disruption of exons 9 and 10 of SPAK. Compared with SPAK^{+/+} littermates, SPAK^{+/-} mice exhibited hypotension without significant electrolyte abnormalities, and SPAK^{-/-} mice not only exhibited hypotension but also recapitulated Gitelman syndrome with hypokalemia, hypomagnesemia, and hypocalciuria. In the kidney tissues of SPAK^{-/-} mice, the expression of total and phosphorylated (p-)NCC was markedly decreased, but that of p-OSR1, total NKCC2, and p-NKCC2 was significantly increased. We observed a blunted response to thiazide but normal response to furosemide in SPAK^{-/-} mice. In aortic tissues, total NKCC1 expression was increased but p-NKCC1 was decreased in SPAK-deficient mice. Both SPAK^{+/-} and SPAK^{-/-} mice had impaired responses to the selective α_1 -adrenergic agonist phenylephrine and the NKCC1 inhibitor bumetanide, suggesting that impaired aortic contractility may contribute to the hypotension of SPAK-null mice. In summary, SPAK-null mice have defects of NCC in the kidneys and NKCC1 in the blood vessels, leading to hypotension through renal salt wasting and vasodilation. SPAK may be a promising target for antihypertensive therapy.

J Am Soc Nephrol 21: 1868–1877, 2010. doi: 10.1681/ASN.2009121295

Sterile 20/SPS1-related proline/alanine-rich kinase (SPAK)^{1,2} and oxidative stress-responsive kinase 1 (OSR1)³ are serine/threonine kinases that share high homology in both their N-terminal catalytic and C-terminal regulatory domains and are widely distributed in the brain, pancreas, heart and kidney.^{2–5} SPAK and OSR1 are downstream substrates of WNK [With-No-Lysine (K)] 1 and 4 kinases and upstream regulators of the cation-chloride co-transporters (Na⁺-K⁺-2Cl⁻ co-transporter [NKCC] 1 and 2 and Na⁺-Cl⁻ co-transporter [NCC]).^{6–9} Specifically, phosphorylation and activation of SPAK and OSR1 by WNK1/4 can in turn phosphorylate and activate NCC/NKCC1.^{10,11}

Gene mutations of the NCC in the distal convoluted tubules (DCTs) and NKCC2 in the thick ascending limb of the loop of Henle (TAL) cause autosomal recessive Gitelman syndrome (GS)¹² and Bartter syndrome (BS),¹³ respectively. These congenital renal tubular disorders are characterized by

Received December 24, 2009. Accepted June 21, 2010.

Published online ahead of print. Publication date available at www.jasn.org.

Correspondence: Dr. Shih-Hua Lin, No. 325, Cheng-Kung Road Section 2, Neihu 114, Taipei, Taiwan. Phone: +886-2-8792-7213; Fax: +886-2-8792-7134; E-mail: l521116@ndmctsgh.edu.tw

Copyright © 2010 by the American Society of Nephrology

renal salt-losing hypotension, secondary hyperreninemia and hyperaldosteronism, and hypokalemic metabolic alkalosis; however, mutations in the *WNK1* and *WNK4* genes cause autosomal dominant pseudohypoaldosteronism type II (PHAII) featuring the mirror image of GS,^{14,15} with salt-sensitive hypertension, low plasma renin activity and inappropriately high plasma aldosterone level, and hyperkalemic metabolic acidosis. A recent human study also showed that genetic variations in the intron regions of *STK39*, the gene encoding SPAK, could enhance its expression and increase susceptibility to hypertension.¹⁶ These findings suggest that SPAK and OSR1 play important roles in BP and renal tubular electrolyte regulation.

We previously found that phosphor (p-) but not total SPAK and OSR1 were increased along with increased total and p-NCC expression in kidneys of *WNK4*^{D561A/+} knock-in mice, recapitulating human PHAII.¹⁷ Conversely, a *WNK4* hypomorphic mouse (by targeting disruption of exon 7 whereby the PHAII-causing mutations are clustered) clearly showed hypotension and decreased expression of p-SPAK/OSR1 and p-NCC.¹⁸ These and other previous findings further reiterate the importance of the *WNK4*-SPAK/OSR1-NCC pathway in the pathogenesis of PHAII.

Because SPAK and OSR1 share high homology in both their catalytic and regulatory domains and their expression in tissues often overlaps, it is crucial to tease apart the role of each kinase. The generation and analysis of individual SPAK- or OSR1-deficient mice may provide better platforms to study this issue. For this purpose, we generated SPAK- and OSR1-null mice by disrupting exons 9 and 10 of the *Stk39* (SPAK) and *Oxsr1* (OSR1) genes, respectively. Homozygous OSR1-null mice died *in utero* as in the recently reported OSR1 gene-trapped mice.¹⁹ We therefore analyzed the SPAK (*Stk39*)-null mice to investigate its role in the kidneys and blood vessels. Results to be reported indicate that SPAK^{-/-} mice exhibited not only hypotension but the phenotype of GS.

RESULTS

Generation of SPAK-Null Mice

To generate SPAK-null mice, we designed a vector to delete exons 9 and 10 of *Stk39* gene (Figure 1A) and 20 homologous recombination embryonic stem (ES) cells were confirmed by Southern blotting (Figure 1B). The neo cassette was excised by transfecting the Flp-expression plasmid into the selected targeted ES cells. We obtained three chimeric mice from two different SPAK^{flox/+} clones and crossed them with C57BL/6 mice to produce SPAK^{flox/+} progeny (Figure 1A). The SPAK^{Δexon 9,10/+} mice were then generated by crossing SPAK^{flox/+} with CAG-Cre recombinase transgenic mice.²⁰ SPAK^{Δexon 9,10/Δexon 9,10} mice were generated by mating SPAK^{Δexon 9,10/+} littermates with each other, and the genotype of the offspring was verified by PCR amplification (Figure 1C). We did not find full-length or estimated hypomorphic (approximately 60 kD) SPAK proteins in either kidneys (Figures 1D and 2A) or aortic tissue,

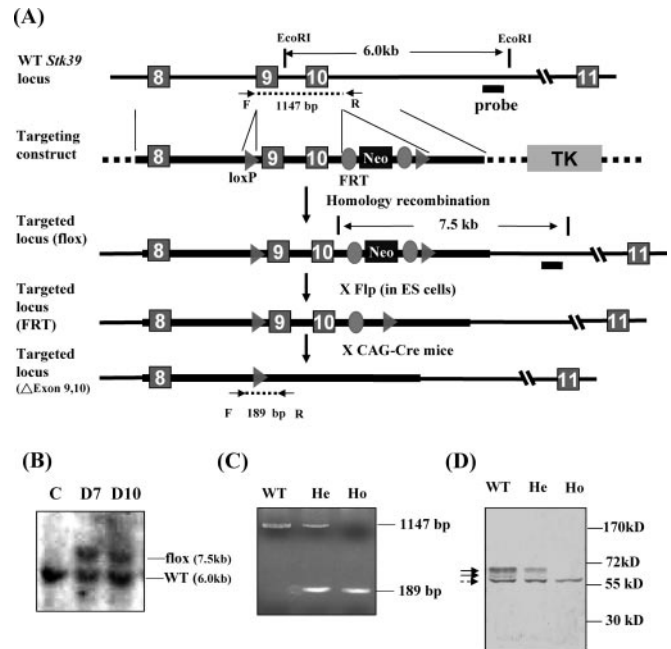


Figure 1. The disruption of exons 9 and 10 of the *Stk39* gene creates SPAK-null mice. (A) Targeting strategy for generating SPAK-null mice. The diagram shows the WT *Stk39* locus encoding SPAK, the targeting construct, and the targeted locus before (flox) and after recombination by Flp (FRT) and Cre (Δ exon 9, 10) recombinase. (B) Verification of homologous recombination by Southern blotting of EcoRI-digested genomic DNA derived from the selected ES cells (D7 and D10) before deleting neomycin transferase (neo) cassette. The 6.0-kb band derives from the WT allele, and the 7.5-kb band derives from the flox allele. C, control genomic DNA from WT ES cells. (C) Genomic DNA derived from tails of SPAK-null mice was used as template, and primers flanking the remaining loxP site (arrow) were used for genotyping. The 189-bp band represents the targeted allele (Δ exon 9 and 10), whereas the 1147-bp band represents the WT allele. C, control genomic DNA from mice. (D) Representative SPAK (arrow) and OSR1 (dashed arrow) protein expression in whole-kidney tissues of WT, SPAK^{+/-} (He), and SPAK^{-/-} (Ho) mice.

confirming that the SPAK protein was not expressed in SPAK^{Δexon 9,10/Δexon 9,10} mice. Hereafter, SPAK^{+/-} and SPAK^{-/-} are used to represent heterozygous (He) and homozygous (Ho) disrupted exons 9 and 10 of *Stk39* gene (SPAK-null) mice, respectively. Because there was no difference in gross appearance and phenotype between D7 and D10 SPAK-null mice strains, the D7 mice were adopted in this study. SPAK^{+/-} and SPAK^{-/-} mice grew normally and were indistinguishable from wild-type (WT) control littermates in appearance, behavior, and fertility.

Phenotype of SPAK-Null Mice

First, we focused on BP and electrolyte homeostasis in the SPAK-null mice. As shown in Table 1, SPAK^{-/-} mice had relative hypotension ($P < 0.05$) and secondary hyperaldosteronism ($P < 0.05$). SPAK^{-/-} mice also exhibited a significant

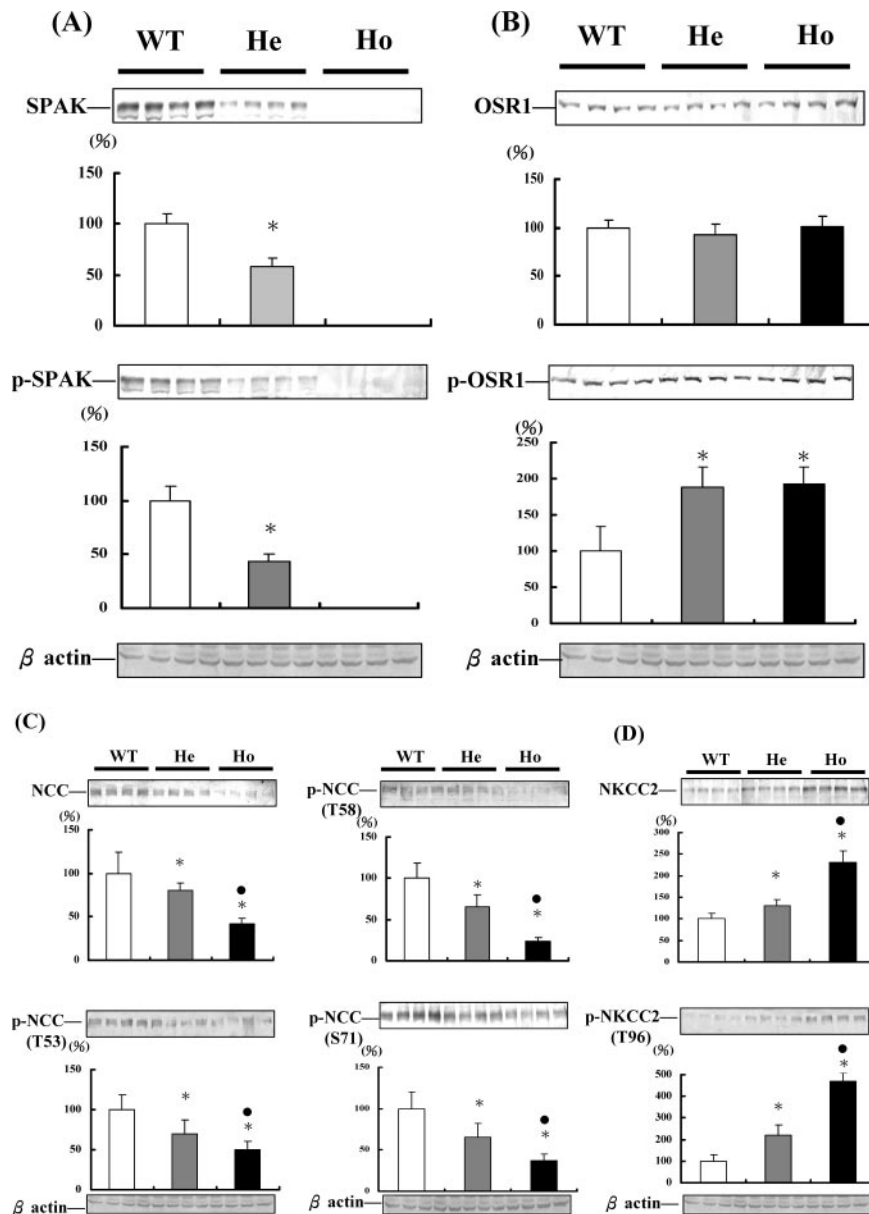


Figure 2. SPAK-null mice have reduced total and p-SPAK, total and p-NCC but increased p-OSR1 and p-NKCC2 expression in kidney tissues. (A through D) Semi-quantitative immunoblotting (top) and densitometry (bottom) of total and p-SPAK (A), total and p-OSR1 (B), total and p-NCC (T53, T58, and S71; C), and total and p-NKCC2 (T96; D) in kidney tissues from WT, SPAK^{+/-} (He), and SPAK^{-/-} (Ho) mice (*n* = 4 per group). **P* < 0.05 versus WT; ●*P* < 0.05 in He versus Ho.

decrease in plasma K⁺ concentration (*P* < 0.05) with increased fractional excretion of K⁺ (FE_K; *P* < 0.05), hypomagnesemia (*P* < 0.01) with increased fractional excretion of Mg²⁺ (FE_{Mg}; *P* < 0.05), and hypocalciuria [Ca²⁺/creatinine 0.12 ± 0.02 versus 0.19 ± 0.03 mg/mg (*n* = 10; *P* < 0.01)]. The failure to develop quite hypokalemia (approximately 3.6 mmol/L) in SPAK^{-/-} mice may be due to their high K⁺ intake per kilogram of body mass (Table 1). Nevertheless, these renal phenotypes resemble the typical clinical features of patients with GS.^{12,21} Conversely, SPAK^{+/-} mice exhibited only relative hypotension

(*P* < 0.05) without significant differences in serum and urine electrolytes, compared with WT controls (Table 1).

Distribution and Expression of SPAK and OSR1 in Renal Tubules

It has been reported that SPAK is distributed in the TAL and DCT¹⁶; however, SPAK^{-/-} mice displayed a GS phenotype corresponding to a DCT lesion with hypocalciuria rather than BS physiology (a TAL lesion with normal-hypercalciuria),²² suggesting predominant distribution and expression of SPAK in DCT. By immunofluorescence (IF) stain in the kidney tissue of WT mice, SPAK was expressed in both the cortex dominantly with co-localization with NCC-positive segment (DCT; Supplemental Figure S1A) and medulla overlapped with NKCC2-positive segment (TAL; Supplemental Figure S1B). OSR1 was widely distributed in the cortex and medulla, including DCT and TAL segments (Supplemental Figure S1C).

Expression of SPAK, OSR1, NKCC2, and NCC in Kidney Tissues

To examine the effect of SPAK deletion on NCC expression, we measured the relative levels of total and p-SPAK and NCC in the kidney tissues by semiquantitative immunoblotting. The lack of total SPAK and p-SPAK (Figure 2A) with markedly reduced total NCC (42 ± 6%; *P* < 0.01) and p-NCC (T53 [50 ± 10%], T58 [24 ± 4%], and S71 [37 ± 8%]; *P* < 0.01) was observed in SPAK^{-/-} mice (Figure 2C). To determine whether the expression of total OSR1 and p-OSR1 was affected in SPAK^{-/-} mice, we also looked at total OSR1, p-OSR1, total NKCC2, and p-NKCC2 (T96; another possible SPAK/OSR1 phosphoacceptor site²³). Although total OSR1 expression was not changed, p-OSR1 (193 ± 22%; *P* < 0.01; Figure 2B), total NKCC2 (230 ± 26%; *P* < 0.01) and p-NKCC2 (T96; 460 ± 37%, *P* < 0.01; Figure 2C) expression were significantly increased.

In the SPAK^{+/-} mice, the expression of SPAK, p-SPAK (Figure 2A), total NCC (80 ± 9%; *P* < 0.05), and p-NCC (T53 [69 ± 18%], T58 [65 ± 14%], and S71 [65 ± 16%]; *P* < 0.01; Figure 2C) were significantly reduced, but the expression of p-OSR1 (188 ± 28%; *P* < 0.01; Figure 2B), NKCC2 (132 ± 14%; *P* < 0.01), and p-NKCC2 (T96; 221 ± 45%; *P* < 0.01; Figure 2D) was significantly increased, compared with WT controls. We also examined the cellular localization and ex-

pression of SPAK, NCC, and NKCC2 in the kidney tissue of SPAK-null mice. The results of IF were consistent with those observed by immunoblotting. As expected, SPAK expression was absent in NCC-positive segment (DCT) in SPAK^{-/-} mice (Supplemental Figure S1A; Figure 3, top right). The cellular distribution of p-NCC (T58) was still lumenally condensed but significantly less in both SPAK^{+/-} and SPAK^{-/-} mice (Figure 3, bottom). Nevertheless, the cellular localization of total NKCC2 and p-NKCC2 (T96) in the TAL was lumenally condensed in SPAK^{+/-} and SPAK^{-/-} mice (Supplemental Figure S2).

Diuretic Response to Hydrochlorothiazide and Furosemide *In Vivo*

We administered hydrochlorothiazide (HCTZ; NCC inhibitor) and furosemide (NKCC2 inhibitor) to determine the NCC and NKCC2 function in these SPAK-null mice. The resulting urine output and Na⁺, K⁺, and Cl⁻ excretion rates were used as an index of NCC and NKCC2 function in response to their inhibitors. Like WT controls, urine amount, FE_{Na}, FE_K, and FE_{Cl} were markedly increased after a single dose of HCTZ treatment in SPAK^{+/-} mice, suggesting that NCC function was still preserved in SPAK^{+/-} mice. Compared with WT and SPAK^{+/-} mice, SPAK^{-/-} mice had a significant decrease in urine amount, FE_{Na}, and FE_{Cl}, supporting that their NCC function was severely diminished (Figure 4A). For NKCC2 function, urine output, FE_{Na}, FE_K, and FE_{Cl} after a single dose of furosemide administration were significantly increased to a

similar extent among WT, SPAK^{+/-}, and SPAK^{-/-} mice (Figure 4B), suggesting that NKCC2 function was still intact in SPAK^{+/-} and SPAK^{-/-} mice.

Expression of SPAK and NKCC1 in Aortic Tissues

Because SPAK and NKCC1 are coexpressed in vascular smooth muscle and NKCC1 activity is known to play an important role in regulation of aortic contractility and BP,^{24,25} we examined whether this pathway could be involved in the hypotension of SPAK-null mice. The relative protein expression of total and p-SPAK/NKCC1 in the aortic tissues of SPAK-null mice were examined. Total SPAK and p-SPAK expression were absent in aortic tissues, akin to the kidneys (Figure 5A). Of interest, we found increased, rather than decreased, total NKCC1 expression in aortic tissues. Nevertheless, the functional p-NKCC1 (T206) was significantly decreased in SPAK^{+/-} and SPAK^{-/-} mice, compared with WT controls (Figure 5B).

Aortic Contractility

To investigate whether the decreased p-NKCC1 (T206) contributed to vasodilation, we evaluated aortic contractility in the SPAK-null mice. The concentration-force relationships for aortic rings of WT controls, SPAK^{+/-} mice, and SPAK^{-/-} mice after stimulation with phenylephrine (PE; a selective α_1 -adrenergic agonist) either in absence or presence of 10 μ M bumetanide (an NKCC1 inhibitor) were examined.²⁴ Without bumetanide, both SPAK^{+/-} and SPAK^{-/-} mice were significantly less responsive to PE stimulation compared with WT control (PE concentration 10⁻⁶ to 10⁻⁴ M; Figure 6A). In the presence of bumetanide, aortic contraction in WT mice was significantly reduced to approximately 50% of maximal contraction (EC50; PE concentration 10⁻⁶ to 10⁻⁴ M; Figure 6B), similar to SPAK^{-/-} and SPAK^{-/-} mice without bumetanide treatment; however, the aortic contractility after bumetanide treatment was significantly reduced only in SPAK^{+/-} but not SPAK^{-/-} mice at PE concentration 10⁻⁴ M (Figure 6, C and D). These findings suggested that impaired NKCC1-mediated aortic contractility may be involved in the hypotension of SPAK-null mice.

DISCUSSION

SPAK-null mice created by targeting disruption of exons 9 and 10 of SPAK (*Stk39*) exhibited low BP and prominent defects in the DCT with GS phenotype, including salt wasting, hypokalemia with renal K⁺ wasting, hypomagnesemia, and hypocalciuria.^{12,21} In the kidneys of SPAK^{-/-} mice, the expression of total and p-NCC in the DCT was markedly decreased but total and p-NKCC2 in the TAL was significantly increased. The aortic tissues in these mice also exhibited a blunted response to PE stimulation and impaired response to bumetanide inhibition, accompanied by decreased p-NKCC1 expression. These results indicate that SPAK is crucial in the regulation of vasoconstriction and renal tubular salt reabsorption.

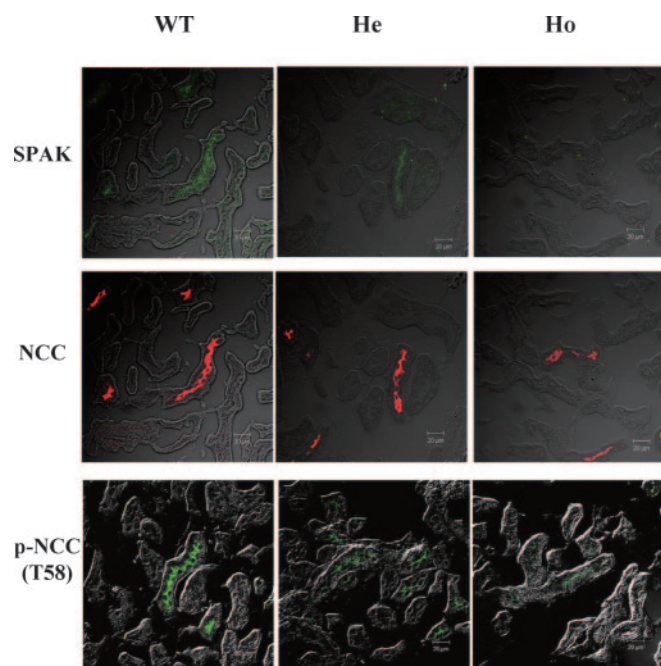


Figure 3. SPAK-null mice have reduced total SPAK, total and p-NCC in kidney tissues by IF stain. Representative IF micrographs of SPAK (top), NCC (middle), and p-NCC (T58; bottom) in the cortex of WT, SPAK^{+/-} (He), and SPAK^{-/-} (Ho) mice. Bar = 20 μ m.

Table 1. BP and blood and urine biochemistries in SPAK-null mice

Parameter	Genotype		
	WT (n = 10)	He (n = 16)	Ho (n = 10)
BP (mmHg)			
systolic	109.5 ± 4.5	95.6 ± 3.6 ^a	93.2 ± 4.1 ^b
diastolic	76.2 ± 5.6	62.1 ± 4.6 ^a	59.3 ± 6.2 ^b
mean	87.2 ± 5.6	74.0 ± 4.5 ^a	71.2 ± 3.5 ^b
Weight (g)	23.8 ± 2.5	23.6 ± 3.3	22.1 ± 1.8
Food intake (g/day per g body wt)	0.07 ± 0.01	0.06 ± 0.02	0.07 ± 0.02
K ⁺ intake (μmol/g per day)	15.1 ± 0.4	14.9 ± 0.6	16.2 ± 0.4
Plasma			
aldosterone (pg/ml)	570 ± 158	707 ± 226	1006 ± 394 ^b
Na ⁺ (mmol/L)	156 ± 3	158 ± 3	157 ± 3
K ⁺ (mmol/L)	4.2 ± 0.3	4.0 ± 0.3	3.6 ± 0.2 ^b
Cl ⁻ (mmol/L)	114 ± 2	113 ± 3	109 ± 2 ^b
total Ca ²⁺ (mg/dl)	9.6 ± 0.2	9.5 ± 0.4	9.7 ± 0.3
Mg ²⁺ (mg/dl)	2.5 ± 0.1	2.3 ± 0.2	1.9 ± 0.2 ^b
BUN (mg/dl)	22.6 ± 4.7	24.2 ± 5.8	27.7 ± 3.5 ^b
Cr (mg/dl)	0.11 ± 0.03	0.12 ± 0.02	0.10 ± 0.02
Urine (ml/day)	1.5 ± 0.4	1.5 ± 0.7	1.6 ± 0.4
CCr (μl/min per g)	8.4 ± 2.2	8.1 ± 1.8	8.6 ± 2.5
pH	6.9 ± 0.9	7.0 ± 0.5	7.1 ± 0.4
Na ⁺ (μmol/day)	97 ± 21	85 ± 25	89 ± 16
K ⁺ (μmol/day)	125 ± 8	124 ± 25	142 ± 22
Cl ⁻ (μmol/day)	85 ± 10	92 ± 11	89 ± 15
FE _{Na} (%)	0.31 ± 0.13	0.32 ± 0.12	0.35 ± 0.15
FE _K (%)	22.4 ± 5.3	24.9 ± 9.6	36.1 ± 7.4 ^b
FE _{Mg} (%)	6.9 ± 1.3	7.3 ± 1.5	9.8 ± 1.2 ^b
Ca ²⁺ /Cr (mg/mg)	0.19 ± 0.03	0.17 ± 0.05	0.12 ± 0.02 ^b

BUN, blood urea nitrogen; CCr, clearance of Cr; Cr, creatinine.

^aP < 0.05, He versus WT.^bP < 0.05, Ho versus WT.

It has been shown that SPAK is expressed in both TAL and DCT of kidney tissues and can activate both NKCC2 and NCC by enhancing their phosphorylation *in vitro* studies.^{8,11,26} It was unclear whether SPAK controlled NKCC2 and/or NCC function *in vivo*. In this study, we found that SPAK was predominantly expressed in the cortex, especially in the DCT; therefore NCC but not NKCC2 would be its major substrate in renal tissues. The expression of total and p-NCC (T53, T58, and S71) but not total and p-NKCC2 (T96) were markedly decreased in SPAK^{-/-} mice, further indicating that NCC is the main target regulated by SPAK. The markedly attenuated NCC but preserved NKCC2 function as evidenced by the blunted response to HCTZ but normal response to furosemide *in vivo* further corroborated that reduced NCC function led to GS phenotype in SPAK^{-/-} mice. The enhanced total and p-NKCC2 expression might be caused by increased p-OSR1 expression in SPAK^{-/-} mice as a compensatory response to loss of NCC function.

NCC in the apical membrane of the DCT mediates reabsorption of 5 to 10% of filtered Na⁺ and is the molecular target of thiazide diuretics.¹² Phosphorylation of NCC by SPAK through a docking interaction between an RFXI motif in the N-terminus of NCC and conserved C-terminal regulatory domain of SPAK^{10,11,19} also participate in maintain-

ing NCC activity without affecting its membrane abundance.²⁶ Among the SPAK phosphoacceptor sites on NCC, the T58 residue plays an important role in triggering NCC activation, and its mutation also abates phosphorylation of the adjacent T44 and T53 sites.²⁷ Human NCC T60M (corresponding to mouse NCC T58M) is one of the most common mutations in Chinese patients with GS.²¹ Because both phosphorylated and total expression of NCC in SPAK^{-/-} mice were markedly diminished, the development of GS was logical. The mode of inheritance of GS is autosomal recessive, but approximately one third of patients with GS are heterozygous or have no detectable NCC mutation.²¹ Given the phenotype of GS in SPAK^{-/-} mice, SPAK, as an upstream regulator of NCC, may be a possible candidate gene for these patients who have GS with only one heterozygous or no detectable NCC mutation. Decreased phosphorylation and abundance of NCC in SPAK-null mice also suggest that the SPAK-NCC signaling cascade may be involved in the sorting or retrieval mechanism of NCC besides affecting NCC phosphorylation and activity found in heterologous expression systems.^{8,26,27}

Reminiscent of the normal BP and absence of GS phenotype in heterozygous NCC knockout mice,²⁸ SPAK^{+/-} mice with >50% total and p-NCC did not have GS phenotype but hypotension. The normal response to HCTZ and furosemide treatment in SPAK^{+/-} mice suggested that their NCC and NKCC2 functions were still conserved. This finding hints that hypotension in SPAK^{+/-} mice may not be primarily caused by reduced NCC function but from other effects. It has been shown that NKCC1, a downstream effector of SPAK/OSR1, can regulate vascular smooth muscle tone. Activation of NKCC1 in blood vessels leads to increased intracellular Cl⁻ concentration, which evokes increased Ca²⁺ influx through L-type Ca²⁺ channels and vessel contraction.^{29–31} Drawing analogy with the reduced BP and vascular tone in NKCC1-null mice,^{24,25} we examined the aortic contractility of SPAK-null mice by PE stimulation, which has also been shown to stimulate vascular contractility by enhanced NKCC1 phosphorylation and activity,³² in the presence and absence of bumetanide. Aortic contractility in both SPAK^{+/-} and SPAK^{-/-} mice was less responsive to PE stimulation. Moreover, impaired bumetanide inhibition of aortic contractility in SPAK^{+/-} and SPAK^{-/-} mice was also observed. Furthermore, p-NKCC1 expression in the aortic tissues of both SPAK^{+/-} and SPAK^{-/-} mice were significantly decreased despite increased total NKCC1 expression. These results suggest that reduced

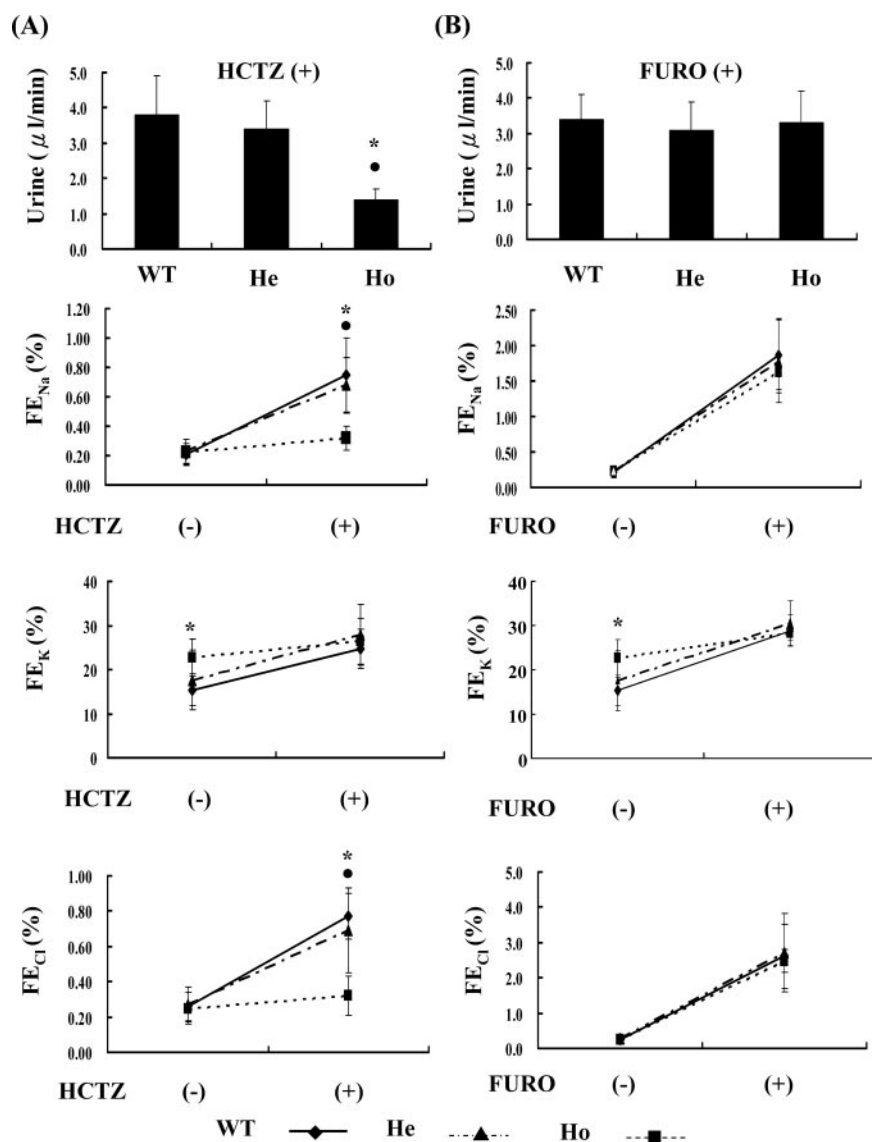


Figure 4. SPAK-null mice show blunted response to HCTZ but normal response to furosemide (FURO). FE_{Na} , FE_{K} , and FE_{Cl} represent the fractional excretion of Na^+ , K^+ , and Cl^- , respectively. (A) Response of urine output, FE_{Na} , FE_{K} , and FE_{Cl} was increased both in WT (◆) and $\text{SPAK}^{+/-}$ (He, ▲) mice but blunted in $\text{SPAK}^{-/-}$ (Ho, ■) mice after HCTZ treatment. (B) All of the WT, $\text{SPAK}^{+/-}$, and $\text{SPAK}^{-/-}$ mice had similar diuretic, FE_{Na} , FE_{K} , and FE_{Cl} response to FURO treatment. *P < 0.05 in WT versus Ho; ●P < 0.05, He versus Ho mice (n = 8 per group).

NKCC1 phosphorylation and function in aortic tissues may contribute to the impaired vasoconstriction and hypotension in these SPAK-null mice, especially in $\text{SPAK}^{+/-}$ mice. In addition to PE, angiotensin II and aldosterone, the activators of the SPAK-NCC cascade in the kidney,^{33–35} have been shown to stimulate aortic contractility *via* activation of NKCC1 in vascular smooth muscle.^{32,36} Whether SPAK acts as an intermediate regulator between these vasoconstrictors and NKCC1 in vascular smooth muscle merits further evaluation.

Thiazides, as an NCC inhibitor, have been widely used clin-

ically as first-line therapy for hypertension. Vasorelaxing agents such as α blockers, Ca^{2+} -channel blockers, angiotensin-converting enzyme inhibitors, and angiotensin II receptor blockers are also commonly used alone or in combination with thiazide diuretics.³⁷ It has been increasingly shown that inhibition of NKCC1 function in smooth muscle, with resulting vasodilation effect, may be an alternative target for treatment of hypertension³⁸; however, the high protein binding of current NKCC1/2 inhibitors (bumetanide and furosemide) means the concentrations required to achieve vasodilation through NKCC1 inhibition will be subjugated first by massive diuresis through NKCC2 inhibition.³⁹ The dual action of SPAK portends the development of SPAK inhibitors, targeting the NCC in the DCT and NKCC1 in vascular smooth muscle, as a novel strategy in anti-hypertensive therapy.

In conclusion, generation and analysis of SPAK-null mice shed light on the important role of SPAK in the vessels and kidneys. The total and p-NCC in the DCT but not NKCC2 in TAL were markedly decreased in $\text{SPAK}^{-/-}$ mice, supporting the notion that NCC is the main target of SPAK and explaining the development of the GS phenotype. Reduced NKCC1 phosphorylation and function in aortic tissues contribute to impaired vasoconstriction and hypotension in these SPAK-null mice (Figure 7). Screening of SPAK gene may be warranted for patients who have GS with only heterozygous or no detectable NCC mutations. SPAK may be a promising target for future antihypertensive therapy.

CONCISE METHODS

Targeted Disruption of SPAK (*Stk39*) Gene

The experimental protocols used in this study were approved by the Institutional Animal Care and Use Committee of the National Defense Medical Center (Taipei, Taiwan). For generation of SPAK-null mice, the targeting vector was prepared by the gap-repair technique.⁴⁰ Mouse *Stk39* genomic DNA encoding SPAK was isolated from a 129/Sv genomic DNA BAC library. The targeting vector was then transfected into R1 ES cells ($129 \times 1/\text{Sv} \times 129\text{S1}$) by electroporation. After selection with 240 $\mu\text{g}/\text{ml}$ G418 and 2 μM gancyclovir, correctly targeted ES clones were selected by Southern blotting. The neo cassette was excised by transfecting the Flp-expression plasmid into the

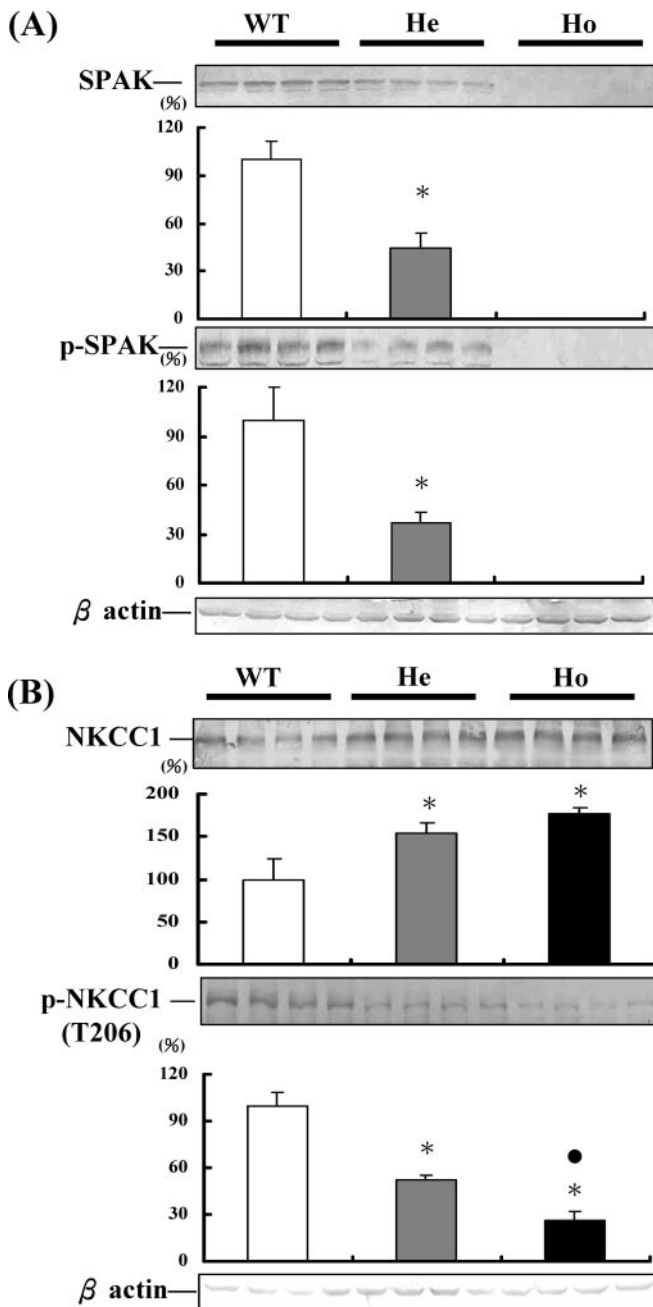


Figure 5. SPAK-null mice have reduced total SPAK, p-SPAK and p-NKCC1 but increased total NKCC1 expression in aortic tissues. (A and B) Semiquantitative immunoblotting (top) and densitometry (bottom) of total and p-SPAK NKCC1 in aortic tissues from WT, SPAK^{+/-} (He), and SPAK^{-/-} (Ho) mice ($n = 4$ per group). * $P < 0.05$ versus WT; ● $P < 0.05$ versus He.

targeted SPAK^{fllox/+} ES cells. The SPAK^{fllox/+} ES cells were again selected by Southern blotting and injected into C57BL/6 blastocysts. Chimeric males were bred with C57BL/6 females to produce heterozygous SPAK^{fllox/+} mice. SPAK^{Δexon 9,10/+} mice were generated by crossing SPAK^{fllox/+} with CAG-Cre recombinase transgenic mice.²⁰ Homozygous SPAK^{Δexon 9,10/Δexon 9,10} mice were then produced by mating SPAK^{Δexon 9,10/+} mice with each other. WT controls and

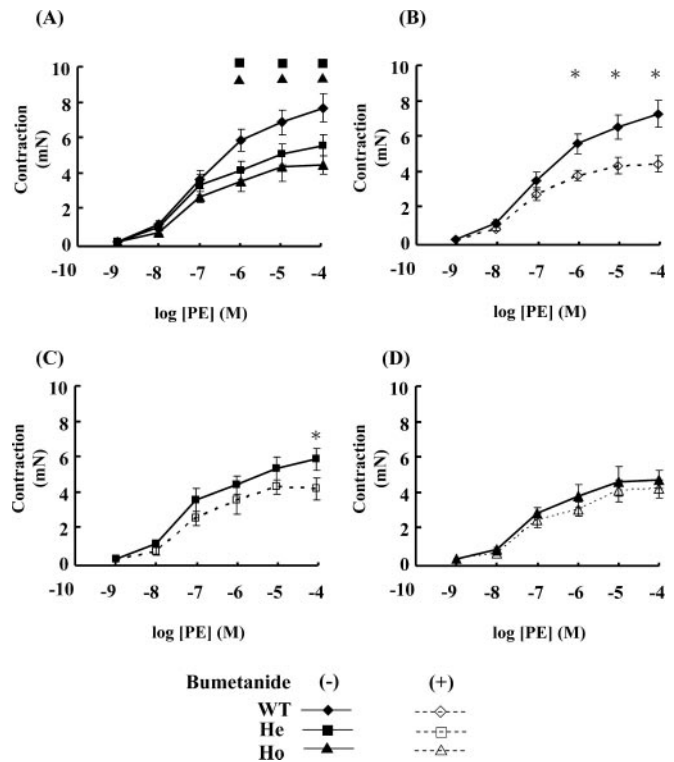


Figure 6. SPAK-null mice show impaired response to phenylephrine (PE)-stimulated aortic contractility and bumetanide inhibition effect. (A through D) Concentration-isometric force relationships for aortic segments in WT, SPAK^{+/-} (He), and SPAK^{-/-} (Ho) mice (A) and bumetanide-sensitive component of aortic contraction in WT (B), He (C), and Ho (D) SPAK-null mice ($n = 6$ per group). ■ $P < 0.05$, WT versus He; ▲ $P < 0.05$, WT versus Ho; * $P < 0.05$, without versus with bumetanide treatment.

SPAK^{Δexon 9,10/+} and SPAK^{Δexon 9,10/Δexon 9,10} littermates were bred and tail genomic DNA was applied for genotyping by PCR (forward primer 5'-GCCAGCACACAACATCTGTC-3'; reverse primer 5'-TAACCTGAAGATGGCTTGC-3'). The mice were raised in a 12-hour day and night cycle, fed with normal rodent diet (Na⁺ 0.3% [wt/wt], K⁺ 1.0% [wt/wt], Ca²⁺ 0.9% [wt/wt]) and plain drinking water *ad libitum*. The phenotype of male mice was evaluated at the age of 12 to 14 weeks.

Blood and Urine Analysis and BP Measurement

Blood was drawn from the submandibular venous plexus under light ether anesthesia. Mice were kept in metabolic cages for urine collection. Plasma creatinine concentration was measured by HPLC assay.⁴¹ Other plasma and urine biochemistries and plasma aldosterone were measured as described previously.²² The BP of restrained conscious mice at steady state was measured with a programmable tail-cuff sphygmomanometer (MK-2000A; Muro-machi, Tokyo, Japan).¹⁷

Generation of p-NKCC Antibody

We generated an antibody to recognize specifically p-NKCC2 on Thr-96 by immunizing rabbits with a keyhole limpet hemocyanin-conjugated synthetic phosphopeptide corresponding to residues 91

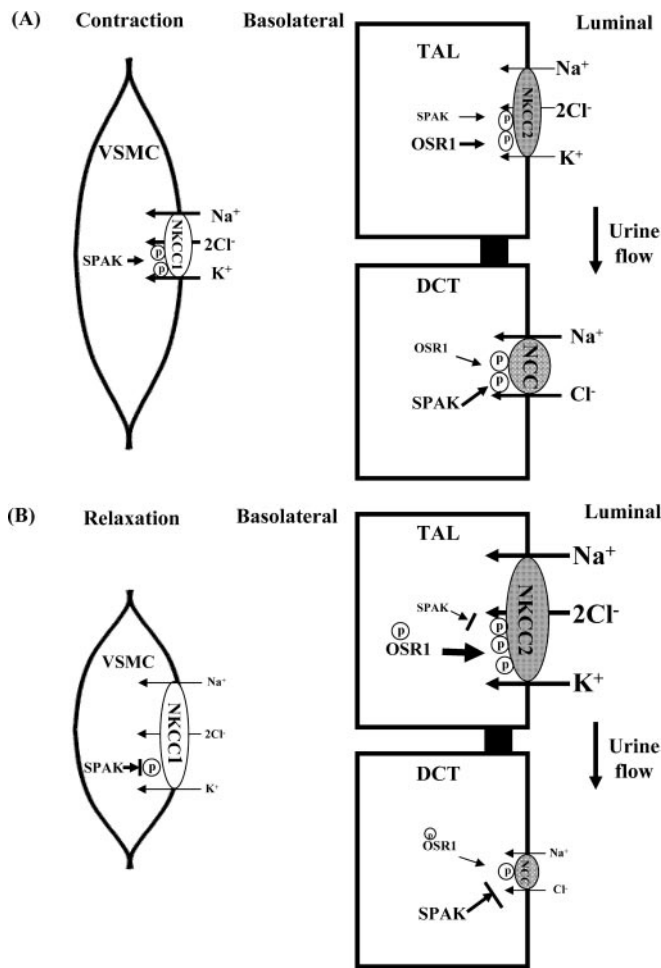


Figure 7. SPAK regulates NKCC1 in vascular smooth muscle and NCC in the kidneys. (A) In renal tubules, phosphorylation of NKCC2 in the TAL and NCC in the DCT are predominantly regulated by OSR1 and SPAK, respectively. In vascular smooth muscle cells (VSMC), SPAK activates the phosphorylation of NKCC1. (B) In SPAK-null mice, reduced phosphorylation and expression of NCC cause defective salt reabsorption in the DCT, leading to GS, with compensatory increased p-OSR1, total NKCC2, and p-NKCC2. Attenuated phosphorylation of NKCC1 results in vasodilation in the VSMC.

through 110 [TYYLQ(pT)FGHN+ Cys] of mouse NKCC2. The serum was affinity-purified with phosphopeptide- and non-phosphopeptide-conjugated cellulose (GenScript, Piscataway, NJ; Supplemental Figure S3). Because of high conservation of the antigen, the antibody also recognizes NKCC1 on Thr-206 [TYYL(pT)FGHN, where R is the only residue that differs between the two sequences provided].

Immunoblotting and IF Stain

Semiquantitative immunoblotting and IF microscopy were carried out as described previously.¹⁷ Relative intensities of the resulting immunoblot band densities were determined by laser scanning (flatbed scanner, GT-12000, EPSON) followed by densitometry using Image J (National Institutes of Health, Bethesda, MD). Densitometry data

were normalized to percentage of lean mean in a double-blinded manner. In addition to our previously generated rabbit anti-p-NCC (T53, T58, and S71),^{17,33} anti-p-OSR1(S325)/SPAK(S383)^{8,18} and newly generated rabbit anti-p-NKCC2 (T96), other commercially available primary antibodies used included rabbit anti-SPAK (Cell Signaling),^{8,16,18} Na-K-2Cl co-transporter 2 (NKCC2; Alpha Diagnostic),⁴² NCC (Chemicon),¹⁷ and mouse anti-OSR1 (Abnova)^{8,18} and NKCC (T4).⁴³ Alkaline phosphatase-conjugated anti-IgG antibodies (Promega) were used as secondary antibodies for immunoblotting, and Alexa 488 or 546 dye-labeled (Molecular Probes) secondary antibodies were used for IF. IF images were obtained using a LSM510 (Carl Zeiss).

HCTZ and Furosemide Treatment

Intraperitoneal HCTZ (12.5 mg/kg) and furosemide (15 mg/kg) were administered, respectively, to the WT mice and SPAK^{+/-} and SPAK^{-/-} littermates.^{17,44} Urine samples in the 4 hours after a single-dose treatment were collected for analysis.

Analysis of Aortic Contractility

Mice were killed by sodium pentobarbital (60 mg/kg, intraperitoneally). The thoracic aortas were quickly removed and placed in Krebs' solution,⁴⁵ then adhering periadventitial tissues were cleaned and cut into segments 2.5 mm in length. The endothelium-denuded aortic rings were mounted in a 10-ml small vessel myograph (Myo-interface Model 610A; Atlanta, GA) organ bath filled with warmed (37°C) oxygenated (95% O₂/5% CO₂) Krebs' solution. The rings were allowed to equilibrate for 1 hour under an optimal resting tension of 1.5 mN. Isometric force was measured with force transducers connected to a PowerLab (AD Instruments, Castle Hill, Australia). After equilibration, PE (1 to 10 nM) concentration-isometric force relationships were generated in the absence and presence of bumetanide (10 μM; 20 minutes of incubation).

Statistical Analysis

All results are expressed as mean ± SD. We used one-way analysis of covariance to compare the differences among the three groups (WT mice and SPAK^{+/-} and SPAK^{-/-} littermates). Paired *t* test was used to compare mice of the same genotype with or without treatment. The Mann-Whitney *U* test was used when the variables between two groups were not normally distributed. *P* < 0.05 was considered to be statistically significant.

ACKNOWLEDGMENTS

This study was supported in part by grants from the National Science Council, Taiwan (NSC 96-2314-B-016-052-MY2; NSC 98-2314-B-016-003-MY3), and by grants from the Research Fund of Tri-Service General Hospital (TSGH-C-98-83 and TSGH-C-99-096), and Japan-Taiwan Joint Research Program, Interchange Association, Japan.

We thank the technical services provided by the Transgenic Mouse Model Core Facility of the National Research Program for Genomic

Medicine, NSC, and Chen-Tzu Chiu for preparation and analysis of aortic contractility.

DISCLOSURES

None.

REFERENCES

- DeAizpurua HJ, Cram DS, Naselli G, Devereux L, Dorow DS: Expression of mixed lineage kinase-1 in pancreatic beta-cell lines at different stages of maturation and during embryonic pancreas development. *J Biol Chem* 272: 16364–16373, 1997
- Johnston AM, Naselli G, Gonez LJ, Martin RM, Harrison LC, DeAizpurua HJ: SPAK, a STE20/SPS1-related kinase that activates the p38 pathway. *Oncogene* 19: 4290–4297, 2000
- Tamari M, Daigo Y, Nakamura Y: Isolation and characterization of a novel serine threonine kinase gene on chromosome 3p22–21.3. *J Hum Genet* 44: 116–120, 1999
- Ushiro H, Tsutsumi T, Suzuki K, Kayahara T, Nakano K: Molecular cloning and characterization of a novel Ste20-related protein kinase enriched in neurons and transporting epithelia. *Arch Biochem Biophys* 355: 233–240, 1998
- Piechotta K, Garbarini N, England R, Delpire E: Characterization of the interaction of the stress kinase SPAK with the Na⁺-K⁺-2Cl[−] cotransporter in the nervous system: Evidence for a scaffolding role of the kinase. *J Biol Chem* 278: 52848–52856, 2003
- Piechotta K, Lu J, Delpire E: Cation chloride cotransporters interact with the stress-related kinases Ste20-related proline-alanine-rich kinase (SPAK) and oxidative stress response 1 (OSR1). *J Biol Chem* 277: 50812–50819, 2002
- Vitari AC, Deak M, Morrice NA, Alessi DR: The WNK1 and WNK4 protein kinases that are mutated in Gordon's hypertension syndrome phosphorylate and activate SPAK and OSR1 protein kinases. *Biochem J* 391: 17–24, 2005
- Moriguchi T, Urushiyama S, Hisamoto N, Iemura S, Uchida S, Natsume T, Matsumoto K, Shibuya H: WNK1 regulates phosphorylation of cation-chloride-coupled cotransporters via the STE20-related kinases, SPAK and OSR1. *J Biol Chem* 280: 42685–42693, 2005
- Vitari AC, Thastrup J, Rafiqi FH, Deak M, Morrice NA, Karlsson HK, Alessi DR: Functional interactions of the SPAK/OSR1 kinases with their upstream activator WNK1 and downstream substrate NKCC1. *Biochem J* 397: 223–231, 2006
- Huang CL, Yang SS, Lin SH: Mechanism of regulation of renal ion transport by WNK kinases. *Curr Opin Nephrol Hypertens* 17: 519–525, 2008
- Richardson C, Alessi DR: The regulation of salt transport and blood pressure by the WNK-SPAK/OSR1 signalling pathway. *J Cell Sci* 121: 3293–3304, 2008
- Simon DB, Nelson-Williams C, Bia MJ, Ellison D, Karet FE, Molina AM, Vaara I, Iwata F, Cushner HM, Koolen M, Gainza FJ, Gitelman HJ, Lifton RP: Gitelman's variant of Bartter's syndrome, inherited hypokalaemic alkalosis, is caused by mutations in the thiazide-sensitive Na-Cl cotransporter. *Nat Genet* 12: 24–30, 1996
- Simon DB, Karet FE, Hamdan JM, DiPietro A, Sanjad SA, Lifton RP: Bartter's syndrome, hypokalaemic alkalosis with hypercalciuria, is caused by mutations in the Na-K-2Cl cotransporter NKCC2. *Nat Genet* 13: 183–188, 1996
- Gordon RD, Hodsman GP: The syndrome of hypertension and hyperkalaemia without renal failure: long term correction by thiazide diuretic. *Scott Med J* 31: 43–44, 1986
- Wilson FH, Disse-Nicodeme S, Choate KA, Ishikawa K, Nelson-Williams C, Desitter I, Gunel M, Milford DV, Lipkin GW, Achard JM, Feely MP, Dussol B, Berland Y, Unwin RJ, Mayan H, Simon DB, Farfel Z, Jeunemaitre X, Lifton RP: Human hypertension caused by mutations in WNK kinases. *Science* 293: 1107–1112, 2001
- Wang Y, O'Connell JR, McArdle PF, Wade JB, Dorff SE, Shah SJ, Shi X, Pan L, Rampersaud E, Shen H, Kim JD, Subramanya AR, Steinle NI, Parsa A, Ober CC, Welling PA, Chakravarti A, Weder AB, Cooper RS, Mitchell BD, Shuldiner AR, Chang YP: From the cover: Whole-genome association study identifies STK39 as a hypertension susceptibility gene. *Proc Natl Acad Sci U S A* 106: 226–231, 2009
- Yang SS, Morimoto T, Rai T, Chiga M, Sohara E, Ohno M, Uchida K, Lin SH, Moriguchi T, Shibuya H, Kondo Y, Sasaki S, Uchida S: Molecular pathogenesis of pseudohypoaldosteronism type II: Generation and analysis of a Wnk4(D561A/+) knockin mouse model. *Cell Metab* 5: 331–344, 2007
- Ohta A, Rai T, Yui N, Chiga M, Yang SS, Lin SH, Sohara E, Sasaki S, Uchida S: Targeted disruption of the Wnk4 gene decreases phosphorylation of Na-Cl cotransporter, increases Na excretion and lowers blood pressure. *Hum Mol Genet* 18: 3978–3986, 2009
- Delpire E, Gagnon KB: SPAK and OSR1: STE20 kinases involved in the regulation of ion homeostasis and volume control in mammalian cells. *Biochem J* 409: 321–331, 2008
- Sakai K, Miyazaki J: A transgenic mouse line that retains Cre recombinase activity in mature oocytes irrespective of the cre transgene transmission. *Biochem Biophys Res Commun* 237: 318–324, 1997
- Lin SH, Shiang JC, Huang CC, Yang SS, Hsu YJ, Cheng CJ: Phenotype and genotype analysis in Chinese patients with Gitelman's syndrome. *J Clin Endocrinol Metab* 90: 2500–2507, 2005
- Cheng CJ, Shiang JC, Hsu YJ, Yang SS, Lin SH: Hypocalciuria in patients with Gitelman syndrome: Role of blood volume. *Am J Kidney Dis* 49: 693–700, 2007
- Rafiqi FH, Zuber AM, Glover M, Richardson C, Fleming S, Jovanovic S, Jovanovic A, O'Shaughnessy KM, Alessi DR: Role of the WNK-activated SPAK kinase in regulating blood pressure. *EMBO Mol Med* 2: 63–75, 2010
- Meyer JW, Flagella M, Sutliff RL, Lorenz JN, Nieman ML, Weber CS, Paul RJ, Shull GE: Decreased blood pressure and vascular smooth muscle tone in mice lacking basolateral Na⁺-K⁺-2Cl[−] cotransporter. *Am J Physiol Heart Circ Physiol* 283: H1846–H1855, 2002
- Garg P, Martin CF, Elms SC, Gordon FJ, Wall SM, Garland CJ, Sutliff RL, O'Neill WC: Effect of the Na-K-2Cl cotransporter NKCC1 on systemic blood pressure and smooth muscle tone. *Am J Physiol Heart Circ Physiol* 292: H2100–H2105, 2007
- Pacheco-Alvarez D, Cristobal PS, Meade P, Moreno E, Vazquez N, Munoz E, Diaz A, Juarez ME, Gimenez I, Gamba G: The Na⁺:Cl[−] cotransporter is activated and phosphorylated at the amino-terminal domain upon intracellular chloride depletion. *J Biol Chem* 281: 28755–28763, 2006
- Richardson C, Rafiqi FH, Karlsson HK, Moleleki N, Vandewalle A, Campbell DG, Morrice NA, Alessi DR: Activation of the thiazide-sensitive Na⁺-Cl[−] cotransporter by the WNK-regulated kinases SPAK and OSR1. *J Cell Sci* 121: 675–684, 2008
- Schultheis PJ, Lorenz JN, Meneton P, Nieman ML, Riddle TM, Flagella M, Duffy JJ, Doetschman T, Miller ML, Shull GE: Phenotype resembling Gitelman's syndrome in mice lacking the apical Na⁺-Cl[−] cotransporter of the distal convoluted tubule. *J Biol Chem* 273: 29150–29155, 1998
- Akar F, Jiang G, Paul RJ, O'Neill WC: Contractile regulation of the Na⁺-K⁺-2Cl[−] cotransporter in vascular smooth muscle. *Am J Physiol Cell Physiol* 281: C579–C584, 2001
- Anfinogenova YJ, Baskakov MB, Kovalev IV, Kilin AA, Dulin NO, Orlov SN: Cell-volume-dependent vascular smooth muscle contraction: Role of Na⁺, K⁺, 2Cl[−] cotransport, intracellular Cl[−] and L-type Ca²⁺ channels. *Pflugers Arch* 449: 42–55, 2004
- Orlov SN, Mongin AA: Salt-sensing mechanisms in blood pressure regulation and hypertension. *Am J Physiol Heart Circ Physiol* 293: H2039–H2053, 2007

32. Akar F, Skinner E, Klein JD, Jena M, Paul RJ, O'Neill WC: Vasoconstrictors and nitrovasodilators reciprocally regulate the Na⁺-K⁺-2Cl⁻ cotransporter in rat aorta. *Am J Physiol* 276: C1383–C1390, 1999
33. Chiga M, Rai T, Yang SS, Ohta A, Takizawa T, Sasaki S, Uchida S: Dietary salt regulates the phosphorylation of OSR1/SPAK kinases and the sodium chloride cotransporter through aldosterone. *Kidney Int* 74: 1403–1409, 2008
34. San-Cristobal P, Pacheco-Alvarez D, Richardson C, Ring AM, Vazquez N, Rafiqi FH, Chari D, Kahle KT, Leng Q, Bobadilla NA, Hebert SC, Alessi DR, Lifton RP, Gamba G: Angiotensin II signaling increases activity of the renal Na-Cl cotransporter through a WNK4-SPAK-dependent pathway. *Proc Natl Acad Sci U S A* 106: 4384–4389, 2009
35. Talati G, Ohta A, Rai T, Sohara E, Naito S, Vandewalle A, Sasaki S, Uchida S: Effect of angiotensin II on the WNK-OSR1/SPAK-NCC phosphorylation cascade in cultured mpkDCT cells and *in vivo* mouse kidney. *Biochem Biophys Res Commun* 393: 844–848, 2010
36. Jiang G, Cobbs S, Klein JD, O'Neill WC: Aldosterone regulates the Na-K-2Cl cotransporter in vascular smooth muscle. *Hypertension* 41: 1131–1135, 2003
37. Moawad MA, Hassan W: Update in hypertension: The Seventh Joint National Committee report and beyond. *Ann Saudi Med* 25: 453–458, 2005
38. Orlov SN: NKCC1 as a regulator of vascular tone and a novel target for antihypertensive therapeutics. *Am J Physiol* 292: H2035–H2036, 2007
39. Hannaert P, Alvarez-Guerra M, Pirot D, Nazaret C, Garay RP: Rat NKCC2/NKCC1 cotransporter selectivity for loop diuretic drugs. *Nauyn Schmiedebergs Arch Pharmacol* 365: 193–199, 2002
40. Liu P, Jenkins NA, Copeland NG: A highly efficient recombineering-based method for generating conditional knockout mutations. *Genome Res* 13: 476–484, 2003
41. Keppler A, Gretz N, Schmidt R, Kloetzer HM, Groene HJ, Lelongt B, Meyer M, Sadick M, Pill J: Plasma creatinine determination in mice and rats: an enzymatic method compares favorably with a high-performance liquid chromatography assay. *Kidney Int* 71: 74–78, 2007
42. Yang SS, Hsu YJ, Chiga M, Rai T, Sasaki S, Uchida S, Lin SH: Mechanisms for Hypercalciuria in pseudohypoaldosteronism type ii-causing WNK4 knock-in mice. *Endocrinology* 151: 1829–1836, 2010
43. Lytle C, Xu JC, Biemesderfer D, Forbush B 3rd: Distribution and diversity of Na-K-Cl cotransport proteins: A study with monoclonal antibodies. *Am J Physiol* 269: C1496–C1505, 1995
44. Lee CT, Chen HC, Lai LW, Yong KC, Lien YH: Effects of furosemide on renal calcium handling. *Am J Physiol* 293: F1231–F1237, 2007
45. Wu CC, Chen SJ, Garland CJ: NO and KATP channels underlie endotoxin-induced smooth muscle hyperpolarization in rat mesenteric resistance arteries. *Br J Pharmacol* 142: 479–484, 2004

See related editorial, "An Emerging Role for SPAK in NCC, NKCC, and Blood Pressure Regulation," on pages 1812–1814.

Supplemental information for this article is available online at <http://www.jasn.org/>.